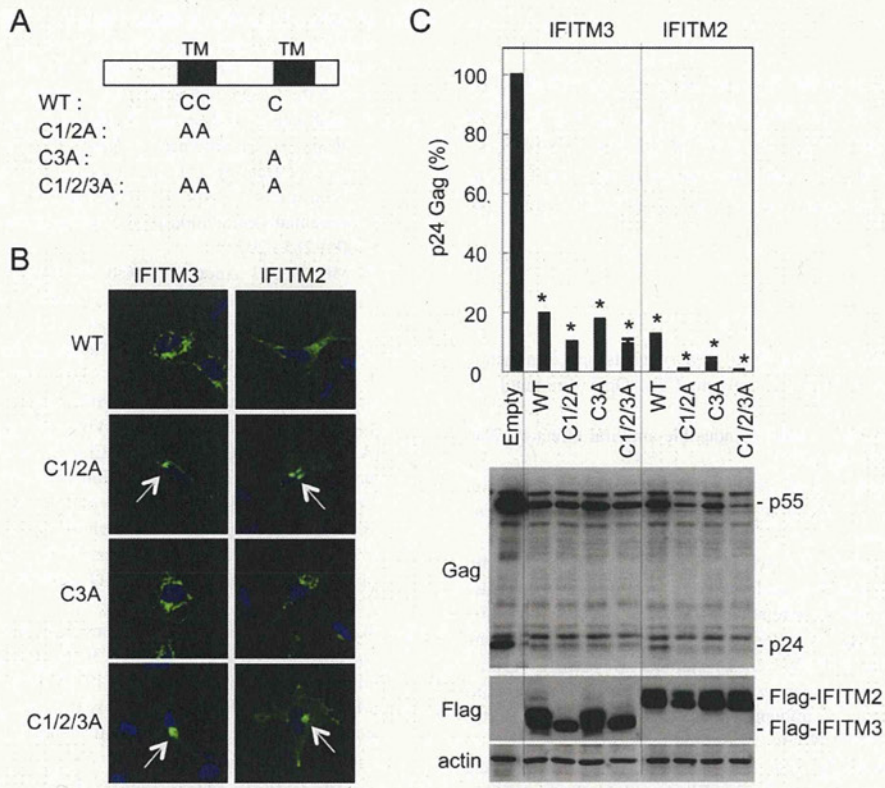

Fig. 6. The effects of S-palmitoylation-deficient IFITM mutants on viral production and Gag expression. (A) The IFITM mutants used are shown schematically. C, cysteine; A, alanine; TM, transmembrane. (B) The 293 cells were transfected with the expression plasmids (1.2 μg) for the wild-type (WT) or three mutants (C1/2A, C3A, and C1/2/3A) of IFITM3 or IFITM2. After 2 days transfection, the cells were fixed and co-stained with DAPI (blue) and anti-Flag antibody to detect Flag-tagged IFITM proteins (green). The C1/2A and C1/2/3A mutants displayed a distinct intracellular distribution (arrows) compared with the WT and C3A mutant. (C) The 293 cells were transfected with the proviral NL43 plasmid (1.0 μg), or co-transfected with the indicated IFITM expression plasmid (0.6 μg). The cells were cultured for 2 days, and the concentration of p24 Gag in the culture supernatants was determined by ELISA (bar graph). The results are expressed as percentages of the value for the sample on the far left. Data are shown as the mean ± SD of triplicate assays. Alternatively, the cells were lysed, and analyzed for the expression of Gag and the Flag-tagged IFITMs by Western blotting (lower blots). The actin blot is a loading control. (B and C) Data shown are representative of two independent experiments with similar results. $^*p < 0.05$. (For interpretation of the references to colour in this figure legend, the reader is referred to the web version of this article.)

cysteines were more heavily S-palmitoylated than the third cysteine [7], the mutants in which the first two cysteines were substituted (C1/2A and C1/2/3A) displayed more marked changes in their intracellular localization (Fig. 6B, arrows). However, unlike in the case of the anti-influenza virus activity of IFITM3, it was found that the S-palmitoylation was not necessary for the anti-HIV-1 activity of IFITMs because all of the mutants of IFITM3 and IFITM2 reduced the concentrations of p24 Gag in the supernatants (Fig. 6C, bar graph) and the expression levels of p55 and p24 Gag proteins in the cells (Gag blot). These results clearly indicated that IFITMs restrict HIV-1 and influenza viruses at distinct steps.

3.5. Conclusion

Both knockdown and enforced expression experiments demonstrated that IFITMs restrict HIV-1 replication [12,13]. In this study, we extended the findings of Lu et al. [12] and revealed that the enforced expression of IFITMs interfered with the production of HIV-1 proteins such as Gag, Vif, and Nef only when viral double-stranded RNAs (RRE and/or TAR) mediated their expression. These findings suggested that IFITM bind directly to viral double-stranded RNA. Indeed, a previous report raised the possibility that IFITM1 is an RRE-binding protein [P. Constantoulakis et al., Inhibition of Rev-mediated HIV-1 expression by an RNA binding protein encoded by the interferon-inducible 9–27 gene, Science 259 (1993) 1314–1318.]. However, as the report was retracted [M. Campbell et al., Science 264 (1994) 492.], careful studies will be necessary in order to clarify the exact mechanisms by which IFITMs interfere with the viral protein expression mediated by the double-stranded viral RNAs such as RRE and TAR. Studies will be also necessary to explain why there was no obvious difference in the anti-HIV-1 activity among three IFITM proteins in our transfection assay, in contrast to the study by Lu et al. [12]. Despite these unanswered questions, the present study demonstrated that IFITMs possess different characteristics from other anti-HIV-1 proteins such as tetherin and APOBEC3G and supported the idea that IFITMs restrict HIV-1 and influenza viruses at distinct steps.

Please cite this article in press as: N. Chutiwitoonchai, et al., Characteristics of IFITM, the newly identified IFN-inducible anti-HIV-1 family proteins, Microbes and Infection (2013), http://dx.doi.org/10.1016/j.micinf.2012.12.003

Acknowledgments

We thank H. Motoyama for her secretarial assistance. This work was supported by the Global COE program "Global Education and Research Center Aiming at the Control of AIDS", which was commissioned by the Ministry of Education, Culture, Sports, Science, and Technology of Japan (to N.C. and S.S.).

References

[1] S.Y. Liu, D.J. Sanchez, G. Cheng, New developments in the induction and antiviral effectors of type I interferon, Curr. Opin. Immunol. 23 (2011) 57–64.

[2] A.J. Sadler, B.R. Williams, Interferon-inducible antiviral effectors, Nat. Rev. Immunol. 8 (2008) 559–568.

[3] R.L. Friedman, S.P. Manly, M. McMahon, I.M. Kerr, G.R. Stark, Transcriptional and posttranscriptional regulation of interferon-induced gene expression in human cells, Cell 38 (1984) 745–755.

[4] S.S. Tanaka, Y.L. Yamaguchi, B. Tsoi, H. Lickert, P.P. Tam, IFITM/Mil/fragilis family proteins IFITM1 and IFITM3 play distinct roles in mouse primordial germ cell homing and repulsion, Dev. Cell 9 (2005) 745–756.

[5] A.L. Brass, I.C. Huang, Y. Benita, S.P. John, M.N. Krishnan, E.M. Feeley, B.J. Ryan, J.L. Weyer, L. van der Weyden, E. Fikrig, D.J. Adams, R.J. Xavier, M. Farzan, S.J. Elledge, The IFITM proteins mediate cellular resistance to influenza A H1N1 virus, West Nile virus, and dengue virus, Cell 139 (2009) 1243–1254.

[6] E.M. Feeley, J.S. Sims, S.P. John, C.R. Chin, T. Pertel, L.M. Chen, G.D. Gaiha, B.J. Ryan, R.O. Donis, S.J. Elledge, A.L. Brass, IFITM3 inhibits influenza A virus infection by preventing cytosolic entry, PLoS Pathog. 7 (2011) e1002337.

[7] J.S. Yount, B. Moltedo, Y.Y. Yang, G. Charron, T.M. Moran, C.B. López, H.C. Hang, Palmitoylome profiling reveals S-palmitoylation-dependent antiviral activity of IFITM3, Nat. Chem. Biol. 6 (2010) 610–614.

[8] D. Jiang, J.M. Weidner, M. Qing, X.B. Pan, H. Guo, C. Xu, X. Zhang, A. Birk, J. Chang, P.Y. Shi, T.M. Block, J.T. Guo, Identification of five interferon-induced cellular proteins that inhibit West Nile virus and dengue virus infections, J. Virol. 84 (2010) 8332–8341.

[9] I.C. Huang, C.C. Bailey, J.L. Weyer, S.R. Radoshitzky, M.M. Becker, J.J. Chiang, A.L. Brass, A.A. Ahmed, X. Chi, L. Dong, L.E. Longobardi, D. Boltz, J.H. Kuhn, S.J. Elledge, S. Bavari, M.R. Denison, H. Choe, M. Farzan, Distinct patterns of IFITM-mediated restriction of filoviruses, SARS coronavirus, and influenza A virus, PLoS Pathog. 7 (2011) e1001258.

[10] J.M. Weidner, D. Jiang, X.B. Pan, J. Chang, T.M. Block, J.T. Guo, Interferon-induced cell membrane proteins, IFITM3 and tetherin, inhibit vesicular stomatitis virus infection via distinct mechanisms, J. Virol. 84 (2010) 12646–12657.

[11] A. Raychoudhuri, S. Shrivastava, R. Steele, H. Kim, R. Ray, R.B. Ray, ISG56 and IFITM1 proteins inhibit hepatitis C virus replication, J. Virol. 85 (2011) 12881–12889.

[12] J. Lu, Q. Pan, L. Rong, S.L. Liu, C. Liang, The IFITM proteins inhibit HIV-1 infection, J. Virol. 85 (2011) 2126–2137.

[13] J.W. Schoggins, S.J. Wilson, M. Panis, M.Y. Murphy, C.T. Jones, P. Bieniasz, C.M. Rice, A diverse range of gene products are effectors of the type I interferon antiviral response, Nature 472 (2011) 481–485.

[14] S.J. Neil, V. Sandrin, W.I. Sundquist, P.D. Bieniasz, An interferon-alpha-induced tethering mechanism inhibits HIV-1 and Ebola virus particle release but is counteracted by the HIV-1 Vpu protein, Cell Host Microbe 2 (2007) 193–203.

[15] S.J. Neil, T. Zang, P.D. Bieniasz, Tetherin inhibits retrovirus release and is antagonized by HIV-1 Vpu, Nature 451 (2008) 425–430.

[16] N. Van Damme, D. Goff, C. Katsura, R.L. Jorgenson, R. Mitchell, M.C. Johnson, E.B. Stephens, J. Guatelli, The interferon-induced protein BST-2 restricts HIV-1 release and is downregulated from the cell surface by the viral Vpu protein, Cell Host Microbe 3 (2008) 245–252.

[17] M. Dubé, B.B. Roy, P. Guiot-Guillain, J. Mercier, J. Binette, G. Leung, E.A. Cohen, Suppression of tetherin-restricting activity upon human immunodeficiency virus type 1 particle release correlates with localization of Vpu in the trans-Golgi network, J. Virol. 83 (2009) 4574–4590.

[18] C. Goffinet, I. Allespach, S. Homann, H.M. Tervo, A. Habermann, D. Rupp, L. Oberbremer, C. Kern, N. Tibroni, S. Welsch, J. Krijnse-Locker, G. Banting, H.G. Kräusslich, O.T. Fackler, O.T. Keppler, HIV-1 antagonism of CD317 is species specific and involves Vpu-mediated proteasomal degradation of the restriction factor, Cell Host Microbe 5 (2009) 285–297.

[19] E. Miyagi, A.J. Andrew, S. Kao, K. Strebel, Vpu enhances HIV-1 virus release in the absence of Bst-2 cell surface down-modulation and intracellular depletion, Proc. Natl. Acad. Sci. U. S. A. 106 (2009) 2868–2873.

[20] K. Chen, J. Huang, C. Zhang, S. Huang, G. Nunnari, F.X. Wang, X. Tong, L. Gao, K. Nikisher, H. Zhang, Alpha interferon potently enhances the anti-human immunodeficiency virus type 1 activity of APOBEC3G in resting primary CD4 T cells, J. Virol. 80 (2006) 7645–7657.

[21] A.M. Sheehy, N.C. Gaddis, J.D. Choi, M.H. Malim, Isolation of a human gene that inhibits HIV-1 infection and is suppressed by the viral Vif protein, Nature 418 (2003) 646–650.

[22] R. Mariani, D. Chen, B. Schröfelbauer, F. Navarro, R. König, B. Bollman, C. Münk, H. Nymark-McMahon, N.R. Landau, Species-specific exclusion of APOBEC3G from HIV-1 virions by Vif, Cell 114 (2003) 21–31.

[23] K. Stopak, C. de Noronha, W. Yonemoto, W.C. Greene, HIV-1 Vif blocks the antiviral activity of APOBEC3G by impairing both its translation and intracellular stability, Mol. Cell 12 (2003) 591–601.

[24] M. Marin, K.M. Rose, S.L. Kozak, D. Kabat, HIV-1 Vif protein binds the editing enzyme APOBEC3G and induces its degradation, Nat. Med. 9 (2003) 1398–1403.

[25] X. Yu, Y. Yu, B. Liu, K. Luo, W. Kong, P. Mao, X.F. Yu, Induction of APOBEC3G ubiquitination and degradation by an HIV-1 Vif-Cul5-SCF complex, Science 302 (2003) 1056–1060.

[26] B. Mangeat, P. Turelli, S. Liao, D. Trono, A single amino acid determinant governs the species-specific sensitivity of APOBEC3G to Vif action, J. Biol. Chem. 279 (2004) 14481–14483.

[27] A. Mehle, B. Strack, P. Ancuta, C. Zhang, M. McPike, D. Gabuzda, Vif overcomes the innate antiviral activity of APOBEC3G by promoting its degradation in the ubiquitin-proteasome pathway, J. Biol. Chem. 279 (2004) 7792–7798.

[28] Y. Iwabu, H. Fujita, M. Kinomoto, K. Kaneko, Y. Ishizaka, Y. Tanaka, T. Sata, K. Tokunaga, HIV-1 accessory protein Vpu internalizes cell-surface BST-2/tetherin through transmembrane interactions leading to lysosomes, J. Biol. Chem. 284 (2009) 35060–35072.

[29] M. Nomaguchi, N. Doi, S. Fujiwara, M. Fujita, A. Adachi, Site-directed mutagenesis of HIV-1 vpu gene demonstrates two clusters of replication-defective mutants with distinct ability to down-modulate cell surface CD4 and tetherin, Front. Microbiol. 1 (2010) 116.

[30] N. Chutiwitoonchai, M. Hiyoshi, P. Mwimanzi, T. Ueno, A. Adachi, H. Ode, H. Sato, O.T. Fackler, S. Okada, S. Suzu, The identification of a small molecule compound that reduces HIV-1 Nef-mediated viral infectivity enhancement, PLoS ONE 6 (2011) e27696.

[31] K.L. Nguyen, M. Ilano, H. Akari, E. Miyagi, E.M. Poeschla, K. Strebel, S. Bour, Codon optimization of the HIV-1 vpu and vif genes stabilizes their mRNA and allows for highly efficient Rev-independent expression, Virology 319 (2004) 163–175.

[32] M. Hiyoshi, S. Suzu, Y. Yoshidomi, R. Hassan, H. Harada, N. Sakashita, H. Akari, K. Motoyoshi, S. Okada, Interaction between Hck and HIV-1 Nef negatively regulates cell surface expression of M-CSF receptor, Blood 111 (2008) 243–250.

[33] R. Hassan, S. Suzu, M. Hiyoshi, N. Takahashi-Makise, T. Ueno, T. Agatsuma, H. Akari, J. Komano, Y. Takebe, K. Motoyoshi, S. Okada, Dys-regulated activation of a Src tyroine kinase Hck at the Golgi disturbs N-glycosylation of a cytokine receptor Fms, J. Cell. Physiol. 221 (2009) 458–468.

[34] T. Chihara, S. Suzu, R. Hassan, N. Chutiwitoonchai, M. Hiyoshi, K. Motoyoshi, F. Kimura, S. Okada, IL-34 and M-CSF share the receptor Fms but are not identical in biological activity and signal activation, Cell Death Differ. 17 (2010) 1917–1927.

Please cite this article in press as: N. Chutiwitoonchai, et al., Characteristics of IFITM, the newly identified IFN-inducible anti-HIV-1 family proteins, Microbes and Infection (2013), http://dx.doi.org/10.1016/j.micinf.2012.12.003

[35] S. Suzu, H. Harada, T. Matsumoto, S. Okada, HIV-1 Nef interferes with M-CSF receptor signaling through Hck activation and inhibits M-CSF bioactivities, Blood 105 (2005) 3230–3237.

[36] J.V. Garcia, A.D. Miller, Serine phosphorylation-independent down-regulation of cell-surface CD4 by nef, Nature 350 (1991) 508–511.

[37] M. Suhasini, T.R. Reddy, Cellular proteins and HIV-1 Rev function, Curr. HIV Res. 7 (2009) 91–100.

[38] Y. Cao, X. Liu, E. De Clercq, Cessation of HIV-1 transcription by inhibiting regulatory protein Rev-mediated RNA transport, Curr. HIV Res. 7 (2009) 101–108.

[39] G. Clerzius, J.F. Gélinas, A. Gatignol, Multiple levels of PKR inhibition during HIV-1 replication, Rev. Med. Virol. 21 (2011) 42–53.

[40] N.V. Jammi, L.R. Whitby, P.A. Beal, Small molecule inhibitors of the RNA-dependent protein kinase, Biochem. Biophys. Res. Commun. 308 (2003) 50–57.

[41] J. Couturier, M. Paccalin, M. Morel, F. Terro, S. Milin, R. Pontcharraud, B. Fauconneau, G. Page, Prevention of the β-amyloid peptide-induced inflammatory process by inhibition of double-stranded RNA-dependent protein kinase in primary murine mixed co-cultures, J. Neuroinflammation 8 (2011) 72.

Please cite this article in press as: N. Chutiwitoonchai, et al., Characteristics of IFITM, the newly identified IFN-inducible anti-HIV-1 family proteins, Microbes and Infection (2013), http://dx.doi.org/10.1016/j.micinf.2012.12.003

Journal of Cellular Physiology

HIV-1 Nef Perturbs the Function, Structure, and Signaling of the Golgi Through the Src Kinase Hck

MASATERU HIYOSHI,[1] NAOKO TAKAHASHI-MAKISE,[1] YUKA YOSHIDOMI,[1] NOPPORN CHUTIWITOONCHAI,[1] TAKASHI CHIHARA,[1] MASATO OKADA,[2] NOBUHIRO NAKAMURA,[3] SEIJI OKADA,[1] AND SHINYA SUZU[1]*

[1]*Center for AIDS Research, Kumamoto University, Kumamoto, Japan*

[2]*Department of Oncogene Research, Research Institute for Microbial Diseases, Osaka University, Osaka, Japan*

[3]*Cell Biology, Division of Life Science, Graduate School of Natural Science and Technologies, School of Pharmacy, College of Medical, Pharmaceutical and Health Sciences, Kanazawa University, Kanazawa, Japan*

The interaction between HIV-1 Nef and the Src kinase Hck in macrophages has been shown to accelerate the progression to AIDS. We previously showed that Nef disturbed the *N*-glycosylation/trafficking of Fms, a cytokine receptor essential for maintaining macrophages in an anti-inflammatory state, in an Hck-dependent manner. Here, we show the underlying molecular mechanism of this effect. Using various Hck isoforms and their mutants and Golgi-targeting Hck mutants, we confirmed that Hck activation at the Golgi causes the Nef-induced Fms *N*-glycosylation defect. Importantly, we found that both the co-expression of Nef and Hck and the expression of a Golgi-targeted active Hck mutant caused alterations in the distribution of GM130, a Golgi protein that was shown to be required for efficient protein glycosylation. Moreover, the activation of Hck at the Golgi caused strong serine phosphorylation of the GM130-interacting Golgi structural protein GRASP65, which is known to induce Golgi cisternal unstacking. Using pharmacological inhibitors, we also found that the activation of Hck at the Golgi followed by the activation of the MAP kinase ERK-GRASP65 cascade is involved in the Fms *N*-glycosylation defect. These results suggest that Nef perturbs the structure and signaling of the Golgi by activating Hck at the Golgi, and thereby, induces the *N*-glycosylation/trafficking defect of Fms, which is in line with the idea that Src family kinases are crucial Golgi regulators.

J. Cell. Physiol. 227: 1090–1097, 2012.

HIV-1 Nef protein is a well-characterized critical determinant of the development of AIDS (Kestler et al., 1991; Deacon, 1995; Kirchhoff et al., 1995). As Nef has no catalytic activity, its pathogenetic function is mediated through cellular machinery (Geyer et al., 2001; Malim and Emerman, 2008). The cellular protein with the highest affinity for Nef is Hck, a Src kinase expressed in macrophages (Saksela et al., 1995; Karkkainen et al., 2006; Trible et al., 2006). Nef induces Hck to adopt a unique active conformation, which allows the constitutive activation of its kinase activity (Moarefi et al., 1997; Lerner and Smithgall, 2002). The pathological importance of the Nef–Hck interaction has been clearly proven by studies with HIV-1 transgenic mice. Mutations in the Hck-binding sites of Nef abolished the development of AIDS-like disease in the HIV-1 transgenic mice (Hanna et al., 1998), and the development of the disease was significantly delayed in the absence of Hck; that is, in $hck^{-/-}$ HIV-1 transgenic mice (Hanna et al., 2001). These findings indicate that the Nef–Hck interaction in macrophages is at least in part responsible for the development of AIDS. This idea was supported by the identification of an unusual Nef variant that failed to activate Hck in a long-term HIV-1-positive non-progressor (Trible et al., 2007). However, it is unclear how this molecular interaction in macrophages affects the progression of the disease.

We previously showed that Nef inhibited M-CSF signaling, the primary cytokine of macrophages (Suzu et al., 2005), by reducing the cell surface expression of the M-CSF receptor Fms (Hiyoshi et al., 2008). The inhibition of the M-CSF–Fms axis may trigger worsening of uncontrolled immune states in HIV-1-infected patients, as M-CSF is essential for maintaining macrophages in an anti-inflammatory state (Hamilton, 2008). We also showed that the reduced surface expression of Fms was due to the accumulation of immature hypo-*N*-glycosylated Fms at the Golgi, which was dependent on the activation of Hck (Hiyoshi et al., 2008). On the other hand, it has been shown that a substantial fraction of Hck is detected at the Golgi and the plasma membrane (Guiet et al., 2008). Nef mainly localizes at the Golgi (Foster and Garcia, 2008), and therefore, the activation of Hck by Nef preferentially occurs at the Golgi (Hung, 2007). Indeed, using various Nef alleles/mutants, we found that the degree of Hck activation at the Golgi was correlated with the degree of impaired intracellular trafficking and *N*-glycosylation of Fms (Hassan, 2009). However, the underlying molecular mechanism responsible for these effects remains to be determined.

The Fms *N*-glycosylation defect induced at the Golgi by the Nef–Hck axis appears to be linked to the idea that Src family kinases play crucial regulatory roles at the Golgi. Src kinases including Hck are involved in an array of signaling pathways involving the plasma membrane (Corey and Anderson, 1999; Lowell, 2004). However, accumulating evidence has suggested

Contract grant sponsor: Ministry of Education, Culture, Sports, Science, and Technology of Japan.

*Correspondence to: Shinya Suzu, Center for AIDS Research, Kumamoto University, Honjo 2-2-1, Kumamoto-city, Kumamoto 860-0811, Japan. E-mail: ssuzu06@kumamoto-u.ac.jp

Received 19 November 2010; Accepted 21 April 2011

Published online in Wiley Online Library (wileyonlinelibrary.com), 12 May 2011.
DOI: 10.1002/jcp.22825

that Src kinases also contribute to the structure and function of the Golgi. Most Src kinases have been physiologically detected at the Golgi (Sallese et al., 2009), and fibroblasts lacking ubiquitous Src kinases (c-Src/Yes/Fyn) exhibited aberrant Golgi structures (Bard et al., 2003). The overexpression of a constitutive-active c-Src mutant resulted in the fragmentation and dispersal of Golgi stacks (Weller et al., 2010). Moreover, an increase in the load of nascent proteins from the endoplasmic reticulum led to the activation of Golgi-localized Src kinases, which regulate protein trafficking activity in secretory pathways (Pulvirenti, 2008). In this study, we therefore analyzed the molecular events, including the signaling cascades, that are induced by the Nef–Hck axis at the Golgi and are involved in the Fms *N*-glycosylation defect.

Materials and Methods

Cells, antibodies, and inhibitors

The HEK293 cells (Invitrogen, Carlsbad, CA) were maintained as described previously (Suzu et al., 2005). The primary antibodies used were as follows: anti-Fms (C-20; Santa Cruz, Santa Cruz, CA), anti-Hck (clone 18; BD Transduction, Lexington, KY), anti-Hck phosphorylated at Tyr 411 (Hck^{pY411}; Santa Cruz), anti-Lyn (clone 42; BD Transduction), anti-c-Src (SRC2; Santa Cruz), anti-CD8 (H-160; Santa Cruz) to detect CD8–Nef fusion proteins (Hiyoshi et al., 2008), anti-ERK1/2 (K-23; Santa Cruz), anti-ERK1/2 phosphorylated at Tyr 204 (E-4; Santa Cruz), anti-GM130 (clone 35; BD Transduction), anti-LAMP-1 (clone 25; BD Transduction), anti-EEA-1 (clone 14; BD Transduction), anti-calnexin (H-70; Santa Cruz), anti-desmoglein (clone 62; BD Transduction), anti-TGN46 (Serotec, Oxford, UK), anti-GRASP65 (CB1011; Calbiochem, Darmstadt, Germany), and anti-GRASP65 phosphorylated at Ser 277 (Yoshimura et al., 2005). PP2 (Sigma, San Diego, CA) and U0126 (Promega, Madison, WI) were used as a Src kinase inhibitor and a MEK/ERK inhibitor, respectively. These inhibitors were dissolved in DMSO (Wako, Osaka, Japan) and added to the cultures at a final concentration of 10 μM.

Plasmids

The human Fms plasmid (pCEF-c-fms) was prepared as described previously (Suzu et al., 2005). The SF2 strain Nef cDNA cloned into the pRc/CMV-CD8 vector was used to express the CD8–Nef fusion protein (Hassan, 2009). Rat GRASP65 cDNA cloned into pcDNA3.1 was prepared as described previously (Yoshimura et al., 2005). Using p56Hck cDNA (Hassan, 2009) as a template, p59Hck cDNA was prepared by PCR. p56Hck-G2A/C3S, p59Hck-G2A, and the constitutive-active (AxxA; Lerner and Smithgall, 2002) and kinase-dead (KE; Lerner and Smithgall, 2002) versions of Hck were prepared using the QuikChange II Site-Directed Mutagenesis Kit (Stratagene, La Jolla, CA). p56Hck-Golgin was prepared by adding cDNA encoding the 184 C-terminal amino acids of Golgin-84, which contain Golgi-retention sequences (Bascom et al., 1999), to the C-terminal end of p56Hck. GalT-p56Hck was prepared by adding cDNA encoding the 81 N-terminal amino acids of GalT (Yamaguchi and Fukuda, 1995), which also contain Golgi-retention sequences, to the N-terminus of p56Hck. All of these cDNA were subcloned into the pcDNA3.1 vector after their nucleotide sequences had been verified. Expression plasmids for Src kinases other than Hck were also used. The murine N-Src plasmid was prepared as described previously (Kotani et al., 2007). Human Fgr in the pApuro2 vector and human Lyn in the pME-puro vector were provided by R. Goitsuka (Tokyo University of Science) and Y. Yamanashi (The University of Tokyo), respectively.

Transfection

Transient transfection of 293 cells was performed as described previously with slight modifications (Hassan, 2009). In brief, cells grown on a 12-well tissue culture plate were transfected with a total of 1.6 μg plasmid using Lipofectamine2000 (Invitrogen). The total amount of plasmids was normalized with empty vectors. After 6 h, the culture medium was replaced with complete DME medium containing 10% FCS. In selected experiments, a kinase inhibitor such as PP2 or U0126 was added to the culture when the medium was changed. The transfected cells were cultured for an additional 42 h and then analyzed by Western blotting, immunofluorescence, and subcellular fractionation.

Western blotting

Total cell lysates were prepared as described previously (Suzu et al., 2000). Cleared cell lysates were resolved by SDS–PAGE under reducing conditions, and the proteins were transferred to a nylon membrane (Hybond-P; GE Healthcare, Buckinghamshire, UK). Detection was performed using ECL Plus Western Blotting Detection Reagents (GE Healthcare) with HRP-labeled anti-immunoglobulin (GE Healthcare). The relative intensity of the bands on scanned gel images was quantified using NIH Image software, and Fms *N*-glycosylation and GRASP65 phosphorylation were also shown graphically using arbitrary units. For Fms *N*-glycosylation, the percentage of immature hypo-*N*-glycosylated Fms (gp130Fms/gp130Fms plus gp150Fms) was calculated and compared among the samples (Hassan, 2009). Data are expressed as fold differences compared with the sample containing the lowest amount of gp130Fms.

Immunofluorescence

For the immunofluorescence, 293 cells were fixed in 2% paraformaldehyde, permeabilized with PBS containing 0.2% Triton X-100 (Hiyoshi et al., 2008), and stained with the primary antibodies (described above) followed by the following secondary antibodies (all from Molecular Probes, Eugene, OR): anti-mouse Alexa Fluor 488, anti-mouse Alexa Fluor 568, anti-rabbit Alexa Fluor 488, and anti-sheep Alexa Fluor 568. Nuclei were also stained with DAPI (Molecular Probes). Fluorescent signals were visualized with a confocal laser scanning microscope LSM 700 (Carl Zeiss, Hamburg, Germany) equipped with 63×/1.4 Oil DIC PlanApochromat objective lenses. Image processing was performed using an LSM software ZEN 2009 (Carl Zeiss).

Subcellular fractionation

The subcellular fractionation on a sucrose gradient was performed exactly as reported previously (Matsuda et al., 2006; Hassan, 2009). In brief, the cells were swollen in hypotonic buffer containing PhoSTOP Phosphatase Inhibitor Cocktail (Roche, Mannheim, Germany) and then homogenized. Then, the post-nuclear supernatants were fractionated by ultracentrifugation (100,000*g* for 75 min) on discontinuous sucrose gradients. All steps were carried out on ice. After ultracentrifugation, the fractions (total 13 fractions) were collected from the tops of the tubes and analyzed by Western blotting with the antibodies described above.

Statistical analysis

The statistical significance of differences between samples was determined using the Student's *t*-test. *P* values less than 0.05 were considered significant.

Results

Hck activation at the Golgi causes the Fms *N*-glycosylation defect

We previously showed that the co-expression of Nef and the p56Hck isoform in 293 cells reduced the cell surface expression of Fms, which was associated with intense Fms signals at the

perinuclear Golgi region and an increase in the expression hypo-*N*-glycosylated gp130Fms (Hiyoshi et al., 2008). Initially, to examine whether the constitutive activation of Hck at the Golgi caused the Fms *N*-glycosylation defect, we tried three different approaches. As Hck is expressed as alternatively translated isoforms (p56Hck and p59Hck) with different lipid modifications (Fig. 1A), we first examined whether the co-expression of Nef with p59Hck also caused the Fms *N*-glycosylation defect. As shown (Fig. 1B), p59Hck/Nef co-expression caused the Fms *N*-glycosylation defect (an increase in the level of gp130Fms), but its level was moderate compared to that induced by p56Hck/Nef co-expression (Fig. 1B, lanes 3 and 4 from the right). This was not due to differences in the degree of activation of these Hck isoforms by Nef, which was assessed by the auto-phosphorylation of Hck at Tyr 411 (Hck^{pY411}; Fig. 1B). Lipid modification is required by both Hck isoforms for the induction of the Fms *N*-glycosylation defect as non-lipid modified mutants (p56Hck-G2A/C3S and p59Hck-G2A; Fig. 1A) had no effect on Fms *N*-glycosylation (Fig. 1B). Based on these findings, we next examined whether the different abilities of these Hck proteins correlated with their presence and activation at the Golgi. An intense signal for Nef-activated p56Hck (Hck^{pY411}) was found at the Golgi region positive for the Golgi protein TGN46 (Fig. 2A, immunofluorescence), and most of the active p56Hck was recovered in fractions containing GM130, another Golgi protein (Fig. 2A, fractionation). In contrast, the signal for Nef-activated p59Hck was detected as small vesicles (Fig. 2B, immunofluorescence), which appeared to overlap with TGN46 (a Golgi marker), LAMP-1 (a lysosome marker), and EEA-1 (an early endosome marker). Indeed, a large proportion of the active p59Hck was recovered in fractions containing EEA-1 (Fig. 2B, fractionation), suggesting its presence in early endosomes. As expected, the non-lipid modified mutants, p56Hck-G2A/C3S and p59Hck-G2A, did not show any specific Golgi-localization, even in the presence of Nef (data not shown). These results support the idea that the presence of active Hck at the Golgi resulted in the Fms *N*-glycosylation defect.

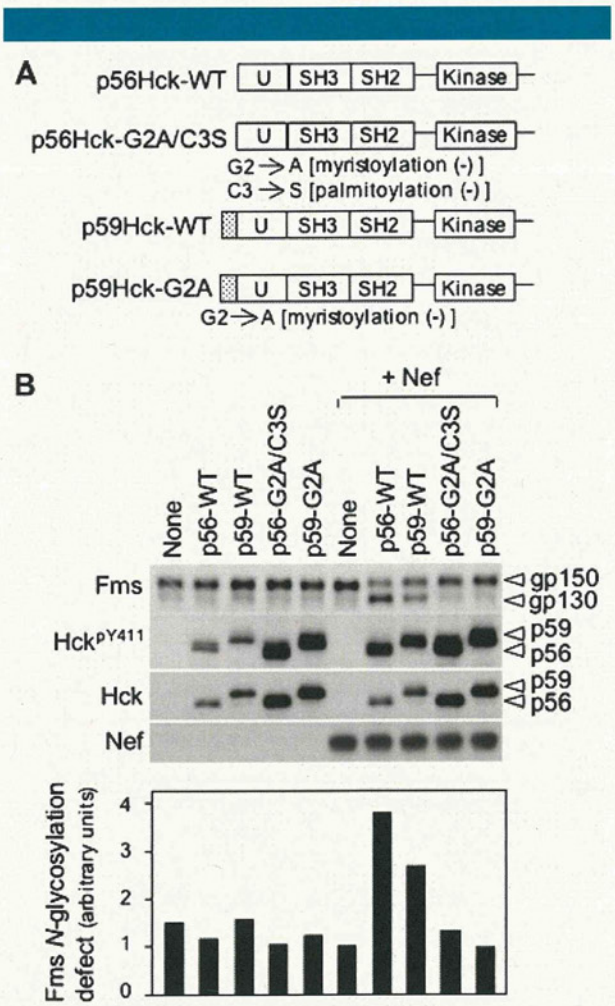

Fig. 1. Different abilities of p56Hck and p59Hck to cause the Fms *N*-glycosylation defect in the presence of Nef. A: The wild-type (WT) p56Hck, p56Hck-G2A/C3S mutant, wild-type (WT) p59Hck, and p59Hck-G2A mutant are schematically shown. p59Hck has 21 additional N-terminal amino acids (Carreno et al., 2000). Both isoforms have a myristoylation site (Gly2), but only p56Hck has a palmitoylation site (Cys3). Thus, the p56Hck-G2A/C3S mutant lacks both myristoylation and palmitoylation sites, whereas the p59Hck-G2A mutant only lacks a myristoylation site. U, unique domain; SH2, Src homology-2 domain; SH3, Src homology-3 domain; kinase, tyrosine kinase domain. B: 293 cells were transfected with the Fms plasmid alone (none) or in combination with the plasmids for Hck and Nef, as indicated. Total cell lysates were subjected to Western blotting with antibodies against Fms, active Hck (Hck^{pY411}), total Hck, and Nef. p56-WT, the wild-type p56Hck; p59-WT, the wild-type p59Hck, p56-G2A/C3S, non-lipid modified p56Hck; p59-G2A, non-lipid modified p59Hck. gp150Fms and gp130Fms are the fully-*N*-glycosylated and hypo-*N*-glycosylated Fms, respectively (Hassan, 2009). Quantified Fms *N*-glycosylation defect values are also shown on the bar graph. The percentage of immature gp130Fms (gp130Fms/gp130Fms + gp150Fms) was calculated and compared among samples. Data are expressed as the fold difference compared with the sample with the lowest amount of gp130Fms. Data shown are representative of three independent experiments with similar results.

We also tested whether other Src kinases had a similar effect on Fms *N*-glycosylation when co-expressed with Nef. Myeloid lineage-specific Src kinases such as Lyn and Fgr were also shown to bind to Nef, but with lower affinity than Hck (Trible et al., 2006). In line with this finding, the degree of the Fms *N*-glycosylation defect induced by Lyn/Nef or Fgr/Nef co-expression was moderate compared with that induced by Hck/Nef expression (Fig. 3A). Interestingly, the neuron-specific Src N-Src induced a severe defect, even when expressed alone (Fig. 3A), and was abundantly detected in the Golgi-like perinuclear region (Fig. 3B). Since it is well known that the kinase activity of N-Src is higher than that of c-Src due to the insertion of six amino acids into the SH3 domain (Cartwright et al., 1987), these results further support the idea that the presence of active Src kinases at the Golgi causes the Fms *N*-glycosylation defect.

We also tested whether the expression of Golgi-targeting Hck mutants was sufficient to cause the Fms *N*-glycosylation defect. p56Hck-Golgin and GalT-p56Hck (Fig. 4A) were prepared by adding the Golgi-retention sequences of Golgin-84 (Bascom et al., 1999) and β-1,4-galactosyltransferase (GalT; Yamaguchi and Fukuda, 1995), respectively. Given the orientation of the Golgi-retention sequences used, p56Hck-Golgin and GalT-p56Hck were expected to face the cytoplasm and the lumen of the Golgi, respectively (Fig. 4A). In addition to the active mutants (AxxA), kinase-dead mutants (KE) were prepared as a control (Fig. 4A). The targeting of these mutants to the Golgi was verified by immunofluorescence (Fig. 4B) and subcellular fractionation analyses (Fig. 4C). As shown in Figure 4D, p56Hck-AxxA-Golgin, which was constitutively active and displayed an endogenous Hck-like orientation, induced a significant Fms *N*-glycosylation defect, even in the absence of Nef. All other mutants including GalT-p56Hck-AxxA, which was also active but faced the Golgi lumen, failed to induce the defect (Fig. 4D). We therefore concluded that the constitutive activation of Src kinases at the Golgi causes the *N*-glycosylation protein defect.

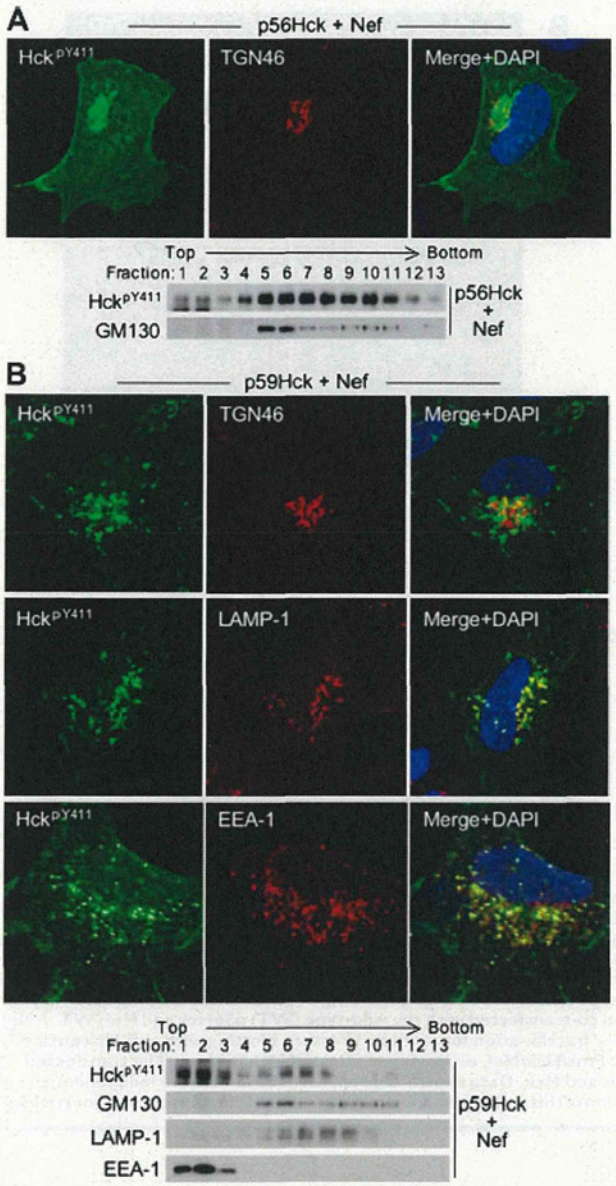

Fig. 2. Difference in intracellular localization between Nef-activated p56Hck and p59Hck. A: 293 cells were transfected with the wild-type p56Hck and Nef plasmids and co-stained with anti-active Hck (Hck^{pY411}, green), anti-TGN46 antibodies (red), and DAPI (blue). The cells were also subjected to subcellular fractionation on a sucrose density gradient followed by Western blotting with antibodies against active-Hck and GM130. A total of 13 fractions were collected from the top of the tube. B: 293 cells were transfected with the wild-type p59Hck and Nef, and analyzed as shown in (A). In Western blotting analysis of the fractions, anti-LAMP-1 and anti-EEA-1 were also used as antibodies for lysosomes and early endosomes, respectively. Data shown are representative of three independent experiments with similar results. [Color figure can be seen in the online version of this article, available at http://wileyonlinelibrary.com/journal/jcp]

Hck activation at the Golgi appears to induce structural changes in the Golgi

We next examined whether the Fms *N*-glycosylation defect caused by Nef/Hck co-expression was associated with structural changes in the Golgi. To this end, we stained co-transfected cells with anti-TGN46 or anti-GM130 antibodies

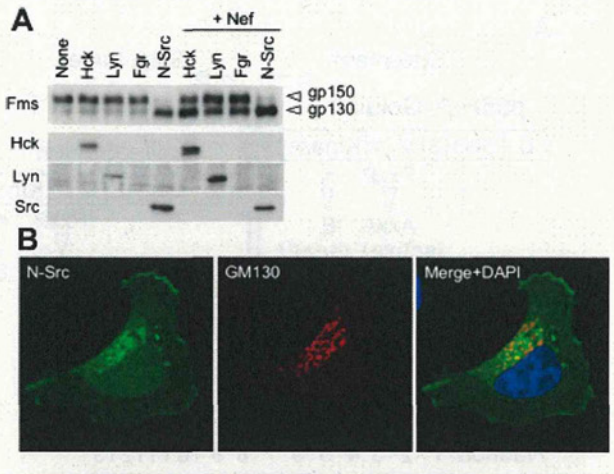

Fig. 3. Effect of the expression of Src kinases on Fms *N*-glycosylation and the intracellular localization of N-Src. A: 293 cells were transfected with Fms alone (none) or in combination with Src kinases (Hck, Lyn, Fgr, or N-Src), as indicated, and analyzed by Western blotting with antibodies against Fms, Hck, Lyn, and Src. gp150Fms and gp130Fms are the fully-*N*-glycosylated and hypo-*N*-glycosylated Fms, respectively. B: 293 cells transfected with N-Src were co-stained with anti-Src antibody (green), GM130 (red), and DAPI (blue). Data shown are representative of three independent experiments with similar results. [Color figure can be seen in the online version of this article, available at http://wileyonlinelibrary.com/journal/jcp]

and compared their staining patterns between active Hck-positive cells and negative cells. As a result, we found that the active Hck-positive cells frequently showed faint TGN46 staining (Fig. 5A, arrows and arrowheads indicate active Hck-positive and negative cells, respectively). Moreover, the active Hck-positive cells frequently showed an unusual staining pattern for another Golgi protein, GM130; that is, compacted staining (Fig. 5B, arrows and arrowheads indicate active Hck-positive and negative cells, respectively). A high percentage of cells showing the compacted GM130 staining was also observed when they were transfected with p56Hck-AxxA-Golgin (Fig. 5C), the Golgi-targeting constitutive-active Hck mutant (see Fig. 4). The change in the intracellular or intra-Golgi distribution of GM130 was further confirmed by quantitative subcellular fractionation. Most GM130 proteins were recovered from the heavy fractions (9, 10, and 11) of untransfected cells (Fig. 6, none). In contrast, the peak of GM130 shifted to lighter fractions in cells transfected with Nef or Hck alone (p56Hck-WT), which was more obvious in the cells co-transfected with Nef and Hck (p56Hck-WT + Nef) and in the cells transfected with p56Hck-AxxA-Golgin. No such change in the peak was observed for calnexin (an endoplasmic reticulum marker) or desmoglein (a plasma membrane marker) (Fig. 6A). These results suggest that Hck activation at the Golgi induces structural changes in the Golgi.

Nef–Hck axis induces the protein *N*-glycosylation defect via the ERK-GRASP65 cascade

As noted above (Figs. 5 and 6), we found a change in the staining pattern of GM130 in active Hck-positive cells. In addition, it has been shown that GM130 binds to and stabilizes a structural Golgi protein, GRASP65 (Barr et al., 1998; Wang et al., 2003). GRASP65 forms oligomers to hold adjacent Golgi cisternae in stacks (Sutterlin et al., 2002; Wang et al., 2003), and the phosphorylation of GRASP65, for example, at serine 277 by the MAP kinase ERK, causes the loss of its oligomerization and

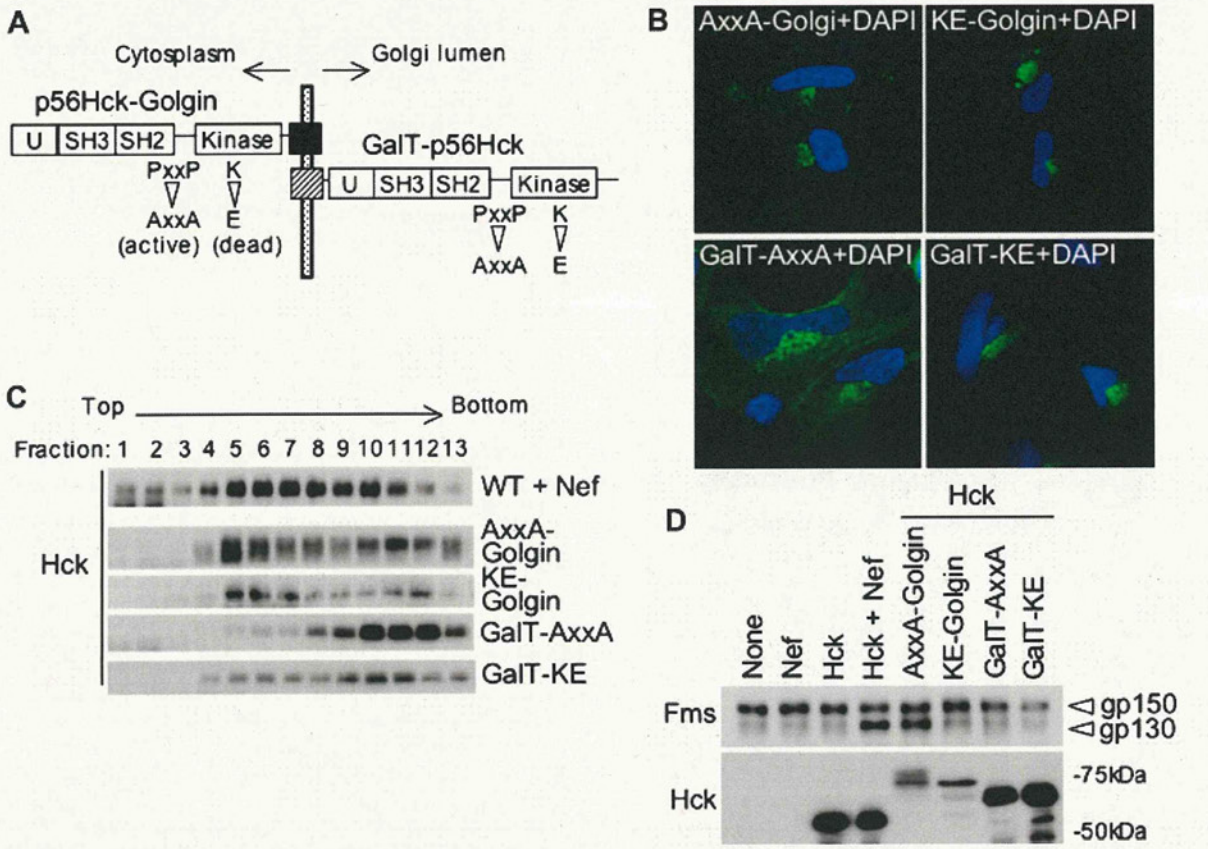

Fig. 4. Effect of Golgi-targeting Hck mutants on Fms *N*-glycosylation. A: Golgi-targeting Hck mutants (p56Hck-AxxA-Golgin, p56Hck-KE-Golgin, GalT-p56Hck-AxxA, and GalT-p56Hck-KE) are schematically shown. p56Hck-Golgin was prepared by adding cDNA encoding the 184 C-terminal amino acids of Golgin-84, which contain Golgi-retention sequences, to the C-terminal end of p56Hck. GalT-p56Hck was prepared by adding cDNA encoding the 81 N-terminal amino acids of GalT, which also contain Golgi-retention sequences, to the N-terminus of p56Hck. AxxA and KE are a constitutive active mutant and a kinase-dead mutant, respectively. B: 293 cells transfected with the indicated Hck plasmid were co-stained with anti-Hck antibody (green) and DAPI (blue). AxxA-Golgin, p56Hck-AxxA-Golgin; KE-Golgin, p56Hck-KE-Golgin; GalT-AxxA, GalT-p56Hck-AxxA; GalT-KE, GalT-p56Hck-KE. C: 293 cells that had been co-transfected with the wild-type (WT) p56Hck and Nef (WT + Nef) or transfected with the indicated Hck mutant were subjected to subcellular fractionation followed by Western blotting with anti-Hck antibody. D: The cells were transfected with Fms alone (none), Fms/Nef, Fms/Hck, Fms/Hck/Nef, or the Fms/indicated Hck mutant. The transfected cells were then analyzed by Western blotting with antibodies against Fms and Hck. Data shown are representative of three independent experiments with similar results. [Color figure can be seen in the online version of this article, available at http://wileyonlinelibrary.com/journal/jcp]

induces Golgi cisternal unstacking (Yoshimura et al., 2005; Bisel et al., 2008; Xiang and Wang, 2010). We therefore hypothesized that the activation of Hck at the Golgi leads to the phosphorylation of GRASP65, and thereby causes the Fms *N*-glycosylation defect. As shown in Figure 7A, we found strong GRASP65 Ser 277 phosphorylation in cells co-transfected with Nef and Hck, as well as in cells transfected with p56Hck-AxxA-Golgin (the Golgi-targeting constitutive active mutant). p56Hck-G2A/C3S-AxxA, which was the constitutively active Hck mutant (Fig. 7A; see Hck^{pY411} blot) but failed to localize in the Golgi due to disruption of its lipid modification sites (data not shown), did not induce any GRASP65 phosphorylation (Fig. 7A). Moreover, the degree of GRASP65 phosphorylation correlated with that of ERK activation (Fig. 7A, AxxA-Golgin > Hck + Nef > G2A/C3S-AxxA; see ERK^{pY204} blot). Of importance, the Src inhibitor PP2 blocked GRASP65 phosphorylation, ERK activation, and Hck activation whereas the MEK/ERK inhibitor U0126 blocked GRASP65 phosphorylation and ERK activation but not Hck activation (Fig. 7B). Finally, both PP2 and U0126 blocked the Nef/Hck-induced Fms *N*-glycosylation defect (Fig. 7C). These results strongly suggest that Nef causes the Fms *N*-glycosylation defect and alters the GM130 distribution by activating the Hck-MEK-ERK-GRASP65 phosphorylation cascade in the Golgi.

Discussion

It is well known that the macrophage-specific cytokine M-CSF is essential for maintaining macrophages in the anti-inflammatory M2 phenotype (Hamilton, 2008). Thus, the *N*-glycosylation/trafficking defect of its receptor Fms by HIV-1 Nef protein may worsen uncontrolled immune states in infected patients (Hiyoshi et al., 2008; Hassan, 2009). In this study, we built on the findings of previous studies and found that the Fms *N*-glycosylation defect induced by the Nef–Hck axis is indeed caused by the activation of Hck at the Golgi and is associated with a change in the distribution of the Golgi protein GM130. Furthermore, we found that the Hck-MEK-ERK-GRASP65 phosphorylation cascade in the Golgi is responsible for inducing the Fms *N*-glycosylation defect.

Our studies with different Hck isoforms and their mutants (Figs. 1 and 2) and Golgi-targeting mutants of Hck (Fig. 4)

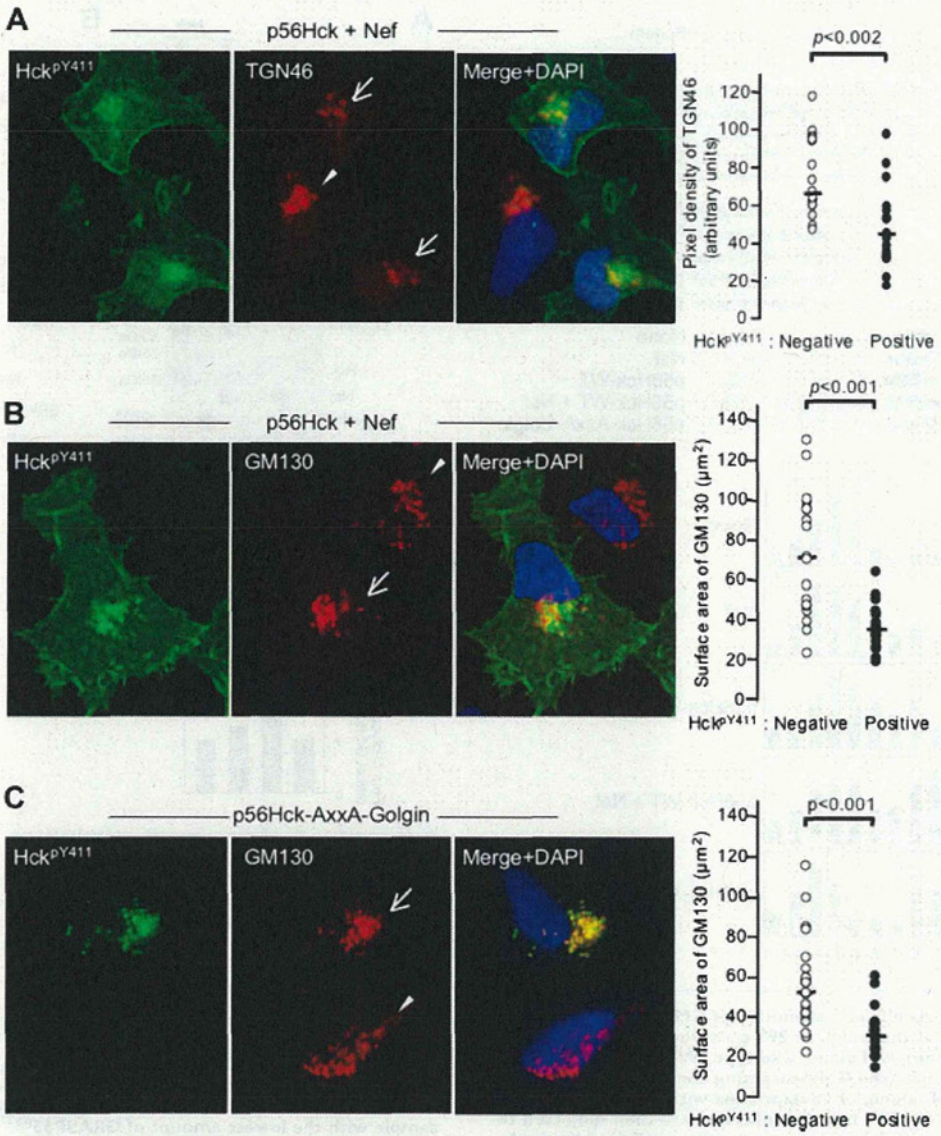

Fig. 5. Altered distributions of TGN46 and GM130 caused by Hck activation at the Golgi. A: 293 cells were co-transfected with p56Hck and Nef and co-stained with anti-active Hck (Hck^{pY411}, green), anti-TGN46 antibodies (red), and DAPI (blue). The arrows and arrowheads indicate the cells positive for active Hck and those negative for active Hck, respectively. In the graph, the pixel density of TGN46 signal was quantified using an NIH ImageJ software 1.42q. The results with the active Hck-negative cells (n = 18) and active Hck-positive cells (n = 15) are shown. Data shown are representative of three independent experiments with similar results. B: 293 cells prepared as in (A) were co-stained with anti-active Hck (Hck^{pY411}, green), anti-GM130 antibodies (red), and DAPI (blue). The arrows and arrowheads indicate the cells positive for active Hck and those negative for active Hck, respectively. In the graph, the surface area of GM130 signal was quantified using an NIH ImageJ software 1.42q. The results with the active Hck-negative cells (n = 18) and active Hck-positive cells (n = 17) are shown. Data shown are representative of three independent experiments with similar results. C: 293 cells were transfected with p56Hck-AxxA-Golgin (the Golgi-targeting constitutive-active mutant; see Fig. 4), co-stained with anti-active Hck (Hck^{pY411}, green), anti-GM130 antibodies (red), and DAPI (blue), and analyzed as shown in (B). The results with the active Hck-negative cells (n = 21) and active Hck-positive cells (n = 19) are shown. Data shown are representative of three independent experiments with similar results. [Color figure can be seen in the online version of this article, available at http://wileyonlinelibrary.com/journal/jcp]

strongly suggest that Nef interferes with the *N*-glycosylation and subsequent cell surface expression of Fms by inducing Hck activation at the Golgi. Our study with N-Src further supported this conclusion (Fig. 3). Interestingly, the above conclusion is consistent with a recent report that growth factor stimulation regulates glycosylation in a Golgi-localized Src kinase-dependent manner (Gill et al., 2010). We also revealed that the constitutive activation of Hck at the Golgi resulted in an altered distribution of Golgi proteins such as TGN46 and GM130 (Figs. 5 and 6), suggesting an altered Golgi structure. Indeed, it was also reported that cells from macaques infected with simian immunodeficiency virus containing HIV-1 Nef exhibit an unusual distribution of Golgi proteins such as p115 and giantin, presumably caused by Hck activation (Sehgal et al., 2009).

One of the noteworthy findings of this study was that GRASP65 was strongly serine phosphorylated downstream of the Hck activation at the Golgi (Fig. 7). It has been shown that GRASP65 is required for Golgi cisternal stacking, and serine

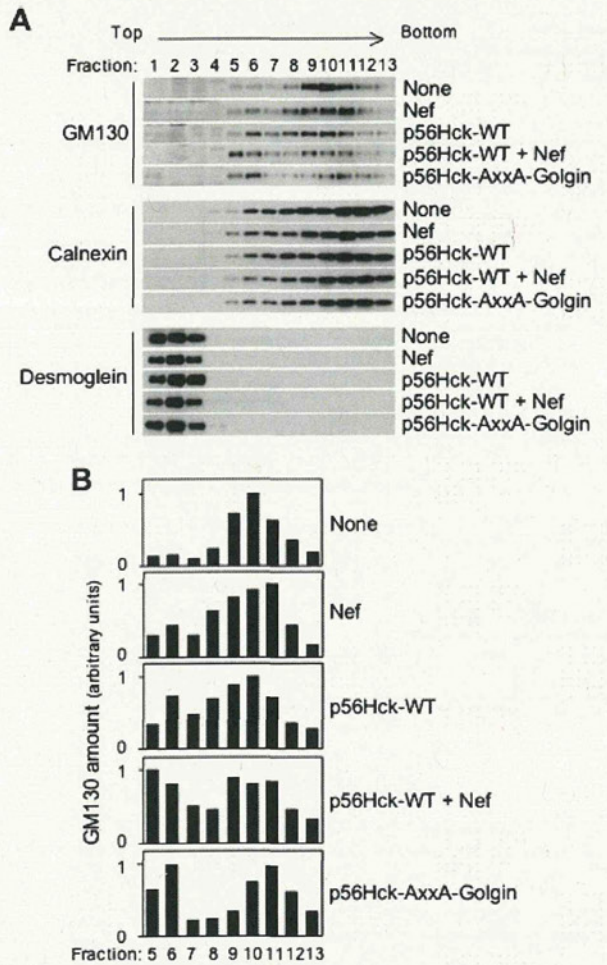

Fig. 6. Altered subcellular distribution of GM130 caused by the activation of Hck at the Golgi. A: 293 cells were transfected with empty vector (none), Nef alone, wild-type (WT) p56Hck alone, p56Hck-AxxA-Golgin (the Golgi-targeting constitutive-active Hck mutant; see Fig. 4) alone, or co-expressed with p56Hck and Nef (p56Hck-WT + Nef). The transfected cells were then subjected to *subcellular fractionation on a sucrose density gradient* followed by Western blotting with antibodies against GM130 and the following marker proteins: calnexin (an endoplasmic reticulum marker) and desmoglein (a plasma membrane marker). A total of 13 fractions were collected from the top of the tube and analyzed. B: The profiles created by quantifying the band pixel densities of GM130 on panel A are shown. Data are expressed as fold differences compared with the fraction containing the highest amount of GM130. Data shown are representative of three independent experiments with similar results.

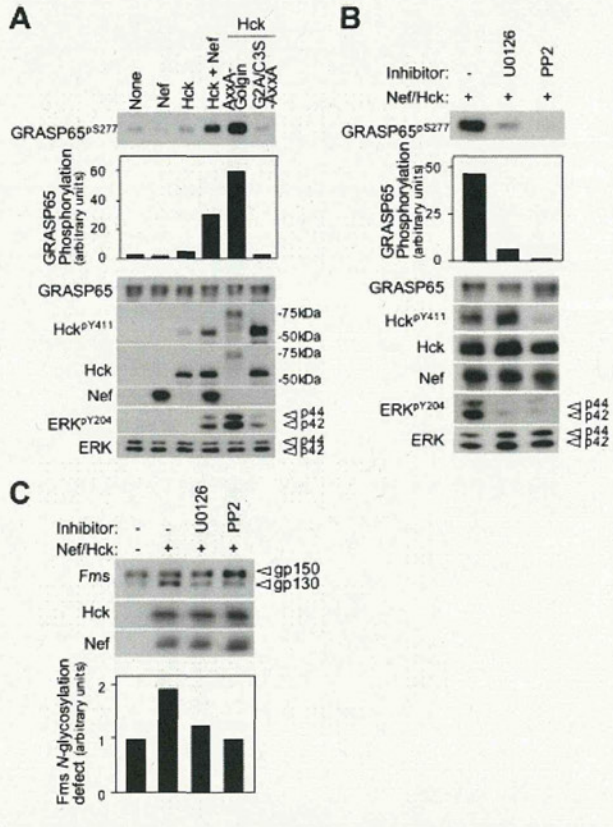

***Fig. 7. Phosphorylation of GRASP65 caused by Hck activation* at the Golgi and the effects of kinase inhibitors on GRASP65 phosphorylation and the Fms *N*-glycosylation defect. A: 293 cells were transfected with GRASP65 alone (none), or co-transfected with Nef, p56Hck, p56Hck/Nef, p56Hck-AxxA-Golgin (the Golgi-targeting constitutive active mutant; see Fig. 4), or p56Hck-G2A/C3S-AxxA (the non-lipid modified constitutive active mutant). The cells were then analyzed by Western blotting with antibodies against phosphorylated GARSP65 (GRASP65^{pS277}), total GRASP65, active-Hck (Hck^{pY411}), total Hck, Nef, active-ERK (ERK^{pY204}), and total ERK. The ERK blot was used as the loading control. The profile created by quantifying the band pixel densities of the GRASP65^{pS277} blot is also shown. Data are expressed as fold differences compared with the sample with the lowest amount of GRASP65^{pS277}. B: 293 cells were co-transfected with GRASP65, p56Hck, and Nef; cultured in the absence or presence of 10 μM U0126 or PP2; and analyzed as shown in (A). C: 293 cells were transfected with Fms alone or co-transfected with Fms, p56Hck, and Nef. Then, the cells were cultured in the absence or presence of 10 μM U0126 or PP2 and analyzed by Western blotting with antibodies against Fms, Hck, and Nef. The quantified Fms *N*-glycosylation defect values are also shown on the bar graph. The percentage of gp130Fms compared with total Fms (gp130Fms and gp150Fms) was calculated, and the data are expressed as fold differences compared with the sample containing the lowest amount of gp130Fms. Data shown are representative of three independent experiments with similar results.**

phosphorylation of GRASP65 causes the loss of its oligomerization and induces Golgi cisternal unstacking (Sutterlin et al., 2002; Yoshimura et al., 2005; Bisel et al., 2008). Stack formation is important for the appropriate localization and function of enzymes that modify oligosaccharides (Kornfeld and Kornfeld, 1985). Indeed, knockdown of GM130, which binds to and stabilizes GRASP65 (Barr et al., 1998; Wang et al., 2003), induces the accumulation of tubulovesicular membranes and cisternal shortening (Marra et al., 2007), inhibits the lateral fusion of Golgi stacks, and disturbs appropriate localization of enzymes that modify oligosaccharides (Puthenveedu et al., 2006). GM130 depletion also causes defective protein sialylation (Puthenveedu et al., 2006), which is consistent with the finding that Nef/Hck co-expression increased the levels of hyposialylated Fms (Hiyoshi et al., 2008). Therefore, our finding that constitutive Hck activation in the Golgi causes GRASP65 phosphorylation (Fig. 7) and altered the distribution of GM130 (Figs. 5 and 6) accounts for the Fms *N*-glycosylation defect induced by the Nef–Hck axis. It remains to be determined which oligosaccharide-modifying enzymes are affected and whether GRASP55, a homologue of GRASP65 (Duran et al., 2008; Feinstein and Linstedt, 2008; Xiang and Wang, 2010), is